INTERACTIONS OF NON-METALLIC INCLUSIONS WITH STEEL AND SLAG: THERMODYNAMIC MODELING, EXPERIMENTS AND METALLOGRAPHIC ANALYSES

Susanne K. Michelic, Mario Hartl, Christian Bernhard,

Chair of Metallurgy, University of Leoben
Franz-Josef-Straße 18, Leoben, 8700, Austria

Keywords: Inclusions, Slags, Thermodynamics, Modification

Abstract

One aspect of an efficient process and product optimization of the liquid steelmaking process is the understanding of reactions and interactions between the components steel, slag and non-metallic inclusions. The present paper focuses on a fundamental study of this topic by combining the powerful methods of thermodynamic modeling with systematic experiments on a laboratory scale and subsequent SEM/EDS analyses. The modeling aspect is addressed by the commercial software FactSage 6.1; laboratory experiments are performed for a low-alloyed, Ca-treated carbon steel combined with varying slag compositions. The consequent SEM/EDS analyses provide a detailed insight into the inclusion landscape which offers a strong tool for characterizing the modification of inclusions. In the present study the combination of these methods is mainly applied to oxides, due to their crucial influence on the final product quality, thus giving important indications for further optimizing the secondary metallurgy processes.

Introduction

In recent years, the range of application for steels has been enlarged continuously; also resulting in extreme surrounding conditions combined with considerable stresses for the material. This trend is directly linked with higher demands on the properties of steels. In order to optimize the final product quality, the cleanness of steels is an important criterion. For this reason, the broad topic “Steel Cleanness” has become one of the main research points at the Chair of Metallurgy. Next to the continuous optimization of methods for the characterization of cleanness, the primary aim is to combine thermodynamic modeling and laboratory experiments in order to describe the changes in inclusion landscape under different conditions.

The steel cleanness can particularly be influenced in the processes of secondary metallurgy. In different processes the reactions and interactions between the components steel, slag and non-metallic inclusions (NMI) are essential for the final inclusion landscape. Consequently, the understanding of the occurring reactions is a fundamental aspect for further development and process optimization. In secondary metallurgy especially oxide-slag systems consisting of the components CaO-Al_2O_3-MgO-SiO_2, which significantly influence the modification of NMI, are of importance. Several works dealing with the interactions of oxide non-metallic inclusions with different slag systems have been published in the last years [1-4]. In order to observe the dissolution of oxides in different slag compositions a Laser Scanning Electron Microscope is frequently used. A very detailed study on the ternary system Al_2O_3-CaO-MgO and its subsystems was also done by De Aza *et al*. [5, 6].

Within the present work, the interactions between the components steel, slag and NMI are considered from a thermodynamic and experimental viewpoint. For the thermodynamic calculations the commercial software FactSage 6.1 is used. The basic approach is the combination of thermodynamic calculations with experiments on laboratory scale followed by automated SEM/EDS analyses. The experimental results with respect to the changes of oxide inclusions within the system CaO-Al_2O_3-MgO due to remelting under three different slag compositions are shown and compared to the calculations.

Methods

Thermodynamic Modeling

The different reactions between steel, slag and NMI under equilibrium conditions were calculated with the "Equilib" tool of FactSage 6.1 using the databases FToxid and FSstel. In a first step, equilibrium calculations of the single components steel, slag and NMI were performed with varying temperature conditions. In a second step, non-metallic inclusions were combined with a steel or slag phase in order to get an impression of their influence on the modification of the NMI. Finally, all components were put together to a complex system as illustrated in Figure 1. As a result a thermodynamic description of the system steel-slag-inclusion for the defined conditions was gained. The calculations done in the present work refer to state 3, always combining 100 g steel with 10 g slag. In the diagrams all components have been normalized.

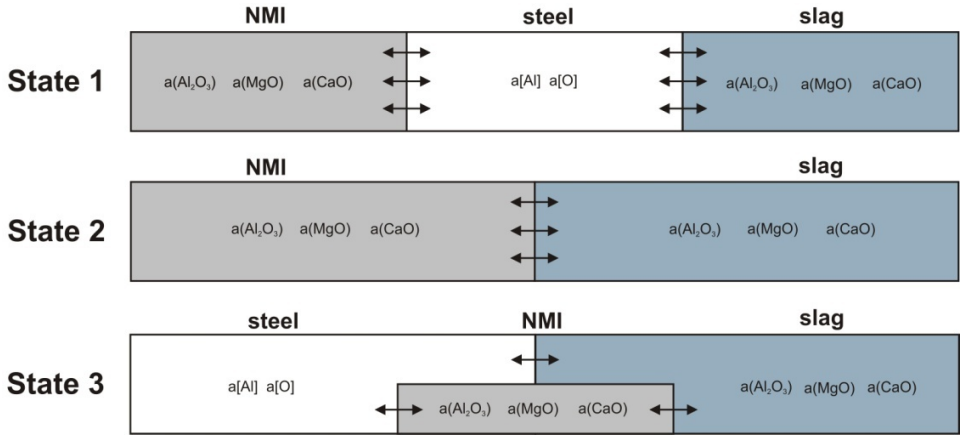

Figure 1. Schematic illustration of the components steel, slag and non-metallic inclusion and possible interactions.

In the present case, a low-alloyed, Ca-treated carbon steel was used for the calculations as well as in the experimental part. This steel was melted in a 20 kg induction furnace; its composition is shown in Table I. Table II summarizes the three different slag compositions which were applied.

To determine the melting ranges of the mentioned slag compositions, the liquid surface projection of the system CaO-Al_2O_3-MgO was calculated as a function of temperature using the "Phase Diagram" module of FactSage 6.1. In Figure 2 two different states are shown for each slag variation:

1. Basic composition of the three slags at room temperature (see also Table I)
2. Composition of the three slags at 1600 °C.

Table I. Steel composition used for thermodynamic modeling and laboratory experiments.

wt.-% C	wt.-% Mn	wt.-% Si	wt.-% Al	wt.-% O
0.16	0.57	0.83	0.021	0.011

Table II. Slag compositions used for thermodynamic modeling and laboratory experiments.

	wt.-% CaO	wt.-% Al_2O_3	wt.-% MgO
Slag 1	50	50	-
Slag 2	20	65	15
Slag 3	33	34	33

It can be seen that in contrast to slag 1, which is part of the binary system CaO-Al_2O_3, slag 2 is saturated with MgO·Al_2O_3 and slag 3 is saturated with MgO. Furthermore, it must be mentioned that the influence of the crucible was only calculated for the case without slag addition. In the calculations with the three different slags, the crucible was not considered.

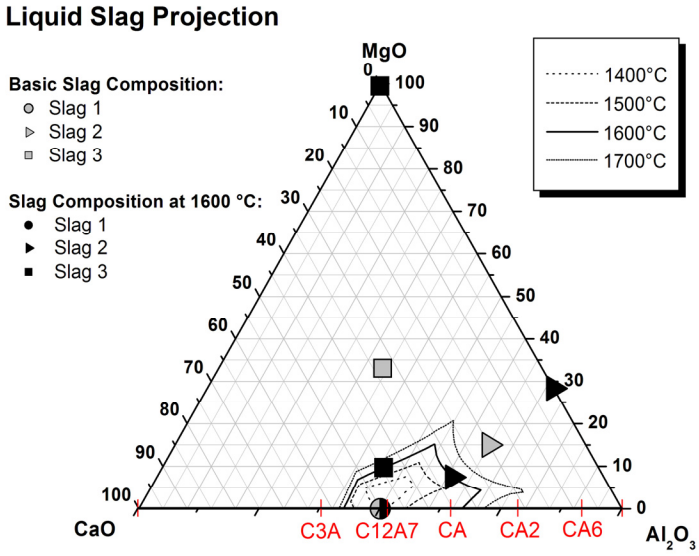

Figure 2. Projection of the liquid slag phase of the system CaO-Al_2O_3-MgO as a function of temperature.

Experiments on Laboratory Scale

In order to validate the calculated results, experiments were performed on a laboratory scale. A low-alloyed, Ca-treated carbon steel was melted in a 20 kg induction furnace (see Table I). The melt was fully deoxidized with Al, a CaFe-wire was used for Ca-treatment, no slag was added during melting. These experimental conditions were chosen consciously, resulting in a relatively high oxygen content compared to industrial processes and therefore a high number of NMI. Samples out of this basic alloy were remelted in a Tammann furnace with additions of different slags. The schematic experimental setup as well as the furnace itself is shown in Figure 3. The Tammann furnace is a high-temperature electric resistance furnace, which can be heated up to 2000 °C. Due to the carbon heating tubes inside the furnace and their reaction with the residual oxygen, the final oxygen content in the furnace vessel is extremely low (0.001 ppm). All experiments were carried out in an Al_2O_3 crucible under Ar-atmosphere (Argon 5.0), using a sample weight of 300 g steel. The samples were heated up to 1600 °C; this temperature was held

for 10 min. In a first phase, the experiment was carried out without slag addition to study the influence of the crucible on the modification of the NMI. In the second phase, the described slags were added to the crucible covering the whole steel bath surface (the slag mass equals appr. 5 % of the steel mass). For every slag, three experiments were performed under the same conditions. After the experiments the steel samples were prepared metallographically and investigated by automated SEM/EDS analyses for the characterization of non-metallic inclusions. The detailed test sequence is shown in Figure 4. Although the possible reaction time in the experiments is comparatively long, only conditions near the equilibrium are obtained. Furthermore, the separation of NMI, and other kinetic aspects – which are not considered in the calculations – influence the resulting inclusion landscape.

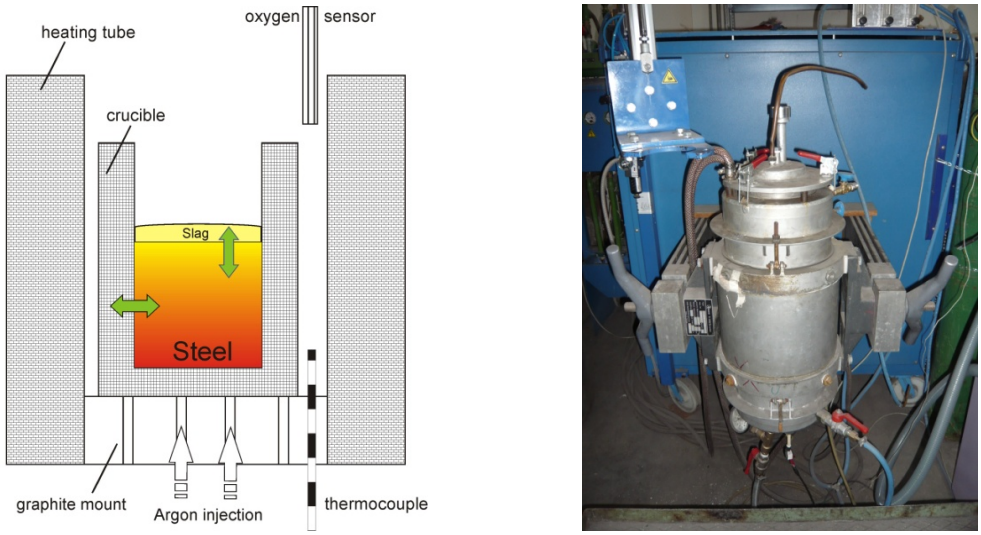

a) b)

Figure 3. a) Schematic illustration and b) photograph of the Tammann furnace used for laboratory experiments.

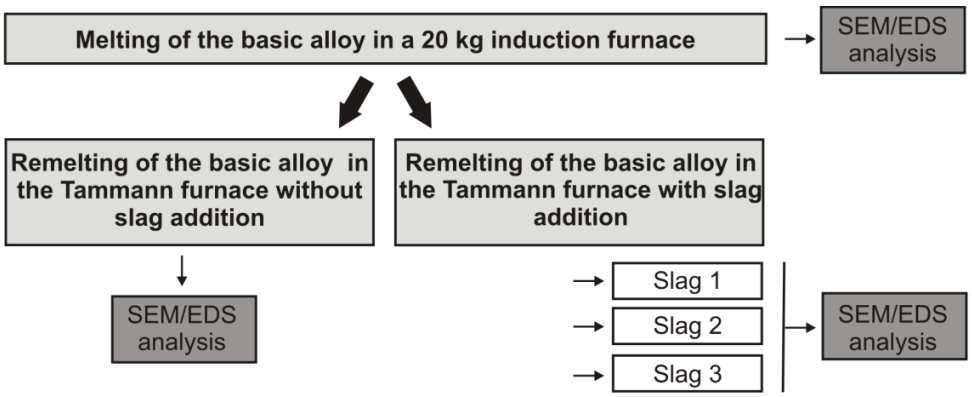

Figure 4. Schematic test sequence.

Metallographic Analyses

For the characterization of non-metallic inclusions by SEM/EDS analysis a polished metallographic specimen is required. Non-metallic inclusions are detected due to material contrast differences in the backscattered electron (BSE) image. The output of automated SEM/EDS analyses regarding the properties of non-metallic inclusions consists of morphological data of every detected particle as well as its chemical composition and the corresponding EDS spectrum.

In addition, in order to get an impression of the sample homogeneity, the distribution of the non-metallic inclusions over the whole sample area is registered. Thus, the possibility of rapidly relocating any particle can be assured, which is a very useful tool in order to manually verify untypical particles after the automated measurement. In general, all inclusion types can be detected simultaneously during the measurement. For the present investigation, a Scanning Electron Microscope manufactured by Fei (Quanta 200 MK2) is used in combination with an EDS system of Oxford Instruments (INCA). In the present study only oxide inclusions (tolerating 2 wt.-% of sulfur at most) are considered in the evaluation. SEM-images giving an overview on detected oxide particles are shown in Figure 5.

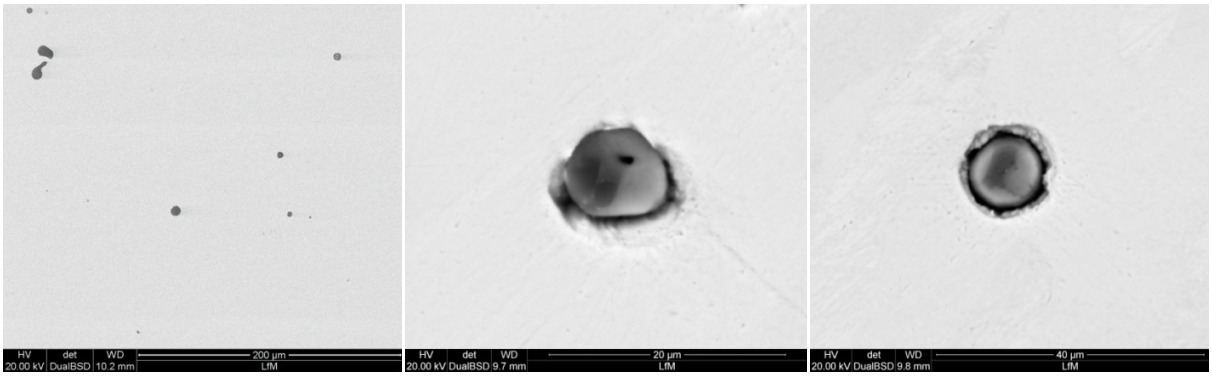

Figure 5. SEM-images of detected oxide non-metallic inclusions – containing Al and Ca – on the analyzed sample area (basic material).

Results and Discussion

The results of the thermodynamic calculations are summarized in Figure 6. The steel and the liquid slag phase as well as the solid oxide components are shown as a function of temperature. On the one hand it is obvious that – as shown in Figure 6a – the contact of the steel with the crucible has a significant influence on the resulting inclusion landscape. A considerable amount of Al_2O_3 inclusions is observed. Regarding the three cases with the addition of different slags, also substantial changes of the non-metallic inclusions' composition are found. While in the case of slag 1 (Figure 6b) mainly CA and C3A are present, for slag 2 and slag 3 multiple solid oxide phases are observed. The calculation with slag 2 leads to a significant amount of $MgO \cdot Al_2O_3$ in the results, which is most likely caused by the presence of this solid phase also at 1600 °C. The same is observed for slag 3, where a nearly constant MgO (s) fraction is found over varying temperature. It seems that these phases – solid at 1600 °C – cannot take part at any reaction in the thermodynamic modeling and therefore remain constant.

The results of the automated SEM/EDS analyses are displayed in Figure 7 and 8. The position of the detected oxides in the ternary system CaO-Al_2O_3-MgO is shown in each case. The initial state of the inclusion landscape, meaning the state before remelting is shown in Figure 7a. Evidently, nearly all oxides are part of the two phase system CaO-Al_2O_3, mainly located at the Al_2O_3 rich side.

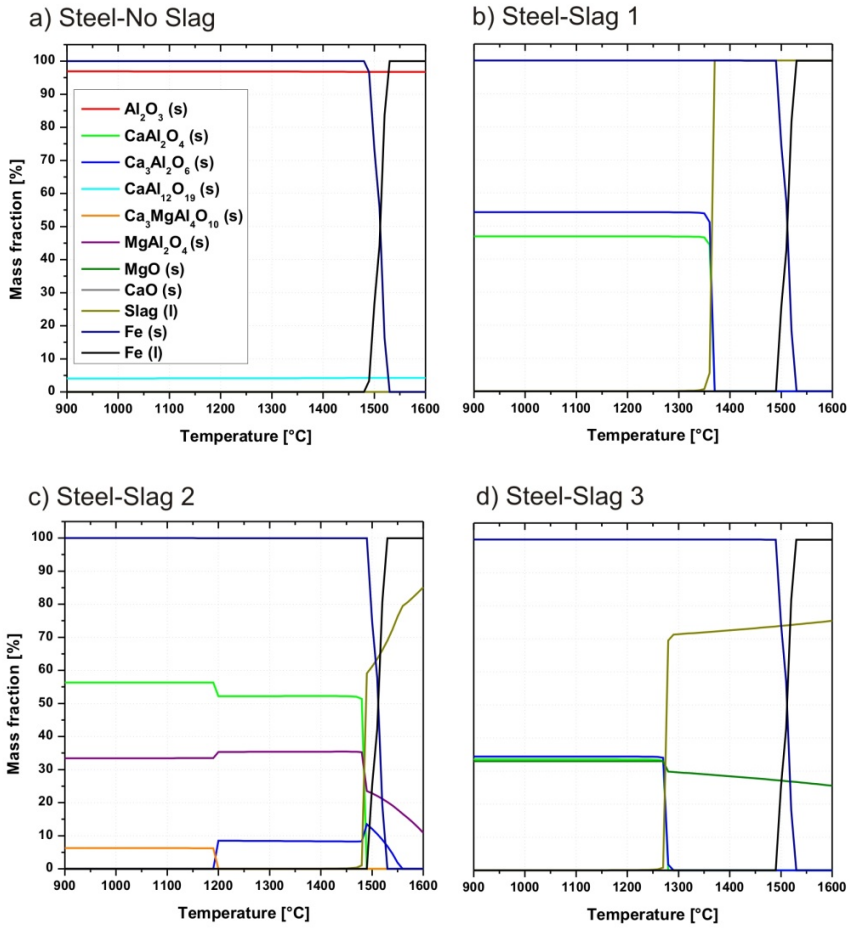

Figure 6. Results of thermodynamic calculations for the different cases.

As displayed in Figure 7b, the remelting of the basic material in the Al_2O_3 crucible leads to a remarkable displacement of the inclusion towards the Al_2O_3 corner. Regarding the results of the experiments with further slag addition (Figure 8), very interesting changes can be observed. While slag 1 does not change the initial state significantly (apart from a slight drift to higher Al_2O_3 contents, which can be attributed to the influence of the crucible), slags 2 and 3 have a higher impact on the resulting inclusion landscape. It must be added that not only the composition of NMI is changed through remelting, but also a significant decrease of the overall number of NMI can be observed.

Due to the high content of Al_2O_3 in slag 2, the inclusions remarkably move towards the Al_2O_3 corner and are finally situated between CA2 and CA6. In contrast to the calculated results, no $MgO{\cdot}Al_2O_3$ are detected in the metallographic analyses. As already mentioned, in this case the calculated solid $MgO{\cdot}Al_2O_3$ are part of the slag phase. This can well be explained by the fact that solid particles in the slag which covering the steel, will hardly interact with the steel owing to the lower density of the steel.

Figure 8c shows the experimental results for slag 3: compared to all other experiments and also in contrast to the calculated results, a significant amount of MgO is present in the inclusions. This inclusion type was found in all experiments using slag 3. A possible explanation may be the reaction of the solved MgO in the slag with the crucible and/or with the steel respectively the

NMI. Pertaining to Figure 2, it can be seen that the content of solved MgO in the slag at 1600 °C is higher for slag 3 than for slag 2 (9.7 vs. 7.5 % solved MgO, respectively). Obviously this slight difference already influences the formation of $MgO{\cdot}Al_2O_3$ according to the above stated mechanism. In addition, comparing the activities of the slag components at 1600 °C (see Table III), it is obvious that in case of slag 2 the $a(Al_2O_3)$ is by far the highest, whereas $a(MgO)\approx 1$ in slag 3, which also gives an indication for the resulting inclusion landscape. To explain the discrepancy between the calculated results and the experimental analyses further investigations are required.

Table III. Activities of the slag components calculated with FactSage 6.1. Reference states are pure solid Al_2O_3, pure solid MgO and pure solid CaO.

	a(CaO)	**$a(Al_2O_3)$**	**a(MgO)**
Slag 1	0.137	0.218	0.000
Slag 2	0.020	0.880	0.058
Slag 3	0.204	0.069	0.995

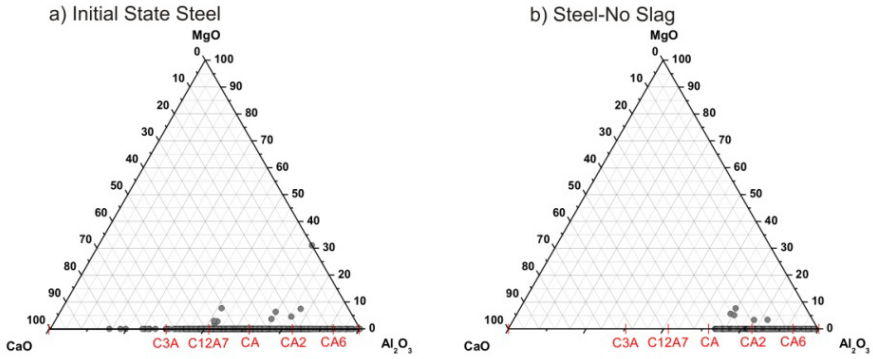

Figure 7. Experimental results of the automated SEM/EDS analyses of a) the initial state in the basic material and b) the remelted alloy without slag addition.

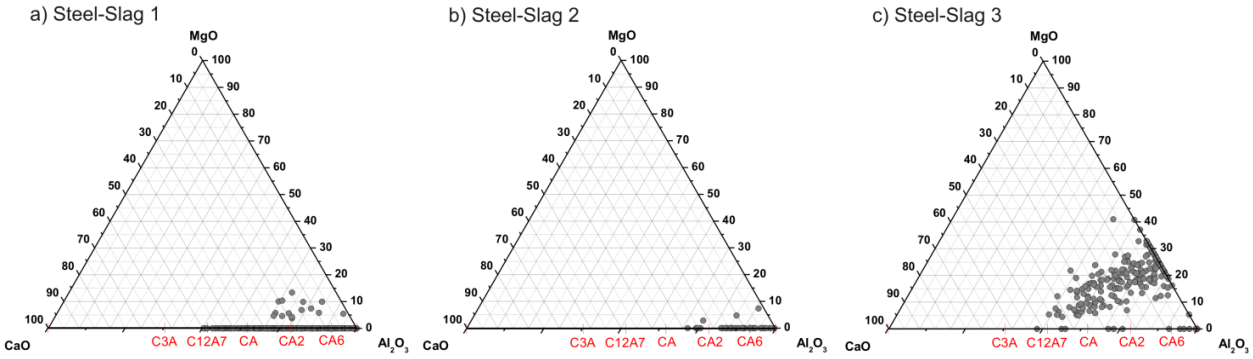

Figure 8. Experimental results of the automated SEM/EDS analyses for the remelted alloy with slag addition: a) slag 1, b) slag 2 and c) slag 3.

Figure 9 shows the modification ratio CaO/Al_2O_3 of the different experimental cases in terms of a scatter band of mean±standard deviation. The figure summarizes the observations made above: Starting from a relatively broad scatter band in the initial state, remelting with slag 1 does not significantly modify the inclusion landscape (apart from the influence of the crucible).

Conversely, remelting with slags 2 and 3 creates inclusions with more Al_2O_3 content; with slag 2 having the greatest influence.

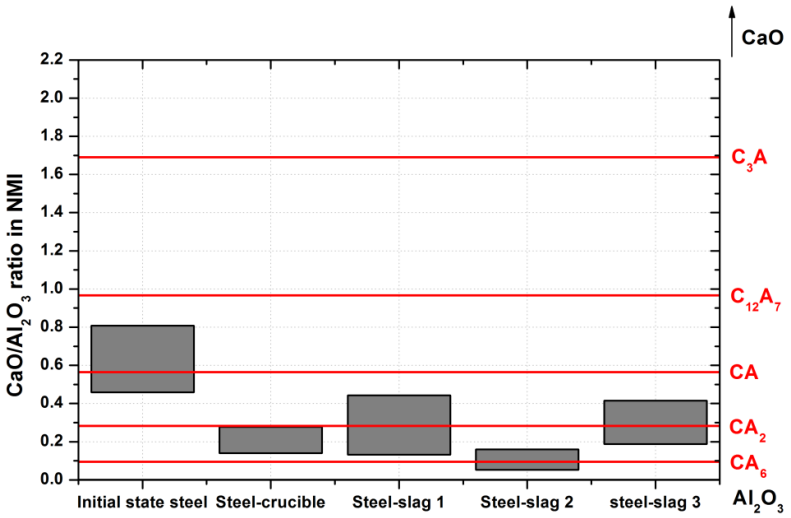

Figure 9. Comparison of modification ratio between the different experimental cases.

Summary and Conclusion

The present paper outlined the comparison of thermodynamic modeling and experimental simulation with subsequent metallographic analysis of the interactions between steel and slag regarding the formation and modification of non-metallic inclusions. Several combinations showed a high degree of conformity between the predictions made by the thermodynamic software FactSage 6.1; on one case a discrepancy was observed which requires further investigation of the occurring mechanisms. Nonetheless, the combination of the methods is highly interesting and yields feasible indications for further process investigations, although not all influences of the experiment can be simulated theoretically. While the present paper only focused on the chemical modification of inclusions, current research activities are also concentrating on the changes in inclusion sizes which is highly important in the processes of secondary metallurgy.

References

1. B.J. Monaghan and L.Chen, "Effect of changing slag composition on spinel inclusion dissolution", *Ironmaking and Steelmaking*, 33 (4) (2006), 323-330.
2. B.J. Monaghan, L.Chen and J. Sorbe, "Comparative study of oxide inclusion dissolution in CaO-SiO_2-Al_2O_3 slag", *Ironmaking and Steelmaking*, 32 (3) (2005), 258-264.
3. M. Valdez et al., "Dissolution of Inclusions in Steelmaking Slags", *ISSTech 2003 Conference Proceedings*, 789-798.
4. K.W. Yi et al., "Determination of dissolution time of Al_2O_3 and MgO inclusions in synthetic Al_2O_3-CaO-MgO slags", *Scandinavian Journal of Metallurgy*, 32 (2003), 177-184.
5. A.H. De Aza, P. Pena and S. De Aza: "Ternary System Al_2O_3-MgO-CaO: I, Primary Phase Field of Crystallization of Spinel in the Subsystem $MgAl_2O_4$-$CaAl_4O_7$-CaO-MgO", *Journal of the American Ceramic Society*, 82 (8) (1999), 2193-2203.
6. A.H. De Aza, P. Pena and S. De Aza: "Ternary System Al_2O_3-MgO-CaO: Part II, Phase Relationship in the Subsystem Al_2O_3-$MgAl_2O_4$-$CaAl_4O_7$", *Journal of the American Ceramic Society*, 83 (4) (2000), 919-927.